433 MHz Lithium Niobate Microbalance Aptamer-Coated Whole Zika Virus Sensor With 370 Hz/ng Sensitivity

Subhashish Dolai and Massood Tabib-Azar, *Senior Member, IEEE*

***Abstract*—Three different microbalances were coated with aptamers with thiol termination designed to attach to the capsid proteins of the whole Zika virus. The first microbalance was a 5 MHz commercial AT-cut (QSense) quartz microbalance that showed 1 Hz/ng sensitivity with minimum detectable signal (MDS) of 1 ng. The second sensor was a 10 MHz AT-cut quartz sensor that was extracted from a communication filter. It had 10 Hz/ng sensitivity and MDS of 0.1 ng. The third sensor was a 433 MHz Lithium Niobate ($LiNbO_3$) sensor that was also extracted from a communication filter. It had 370 Hz/ng sensitivity and 2.7 pg MDS. These studies verify binding of the aptamers to the sensor surface and the Zika virus. They also clearly show the advantage of using the $LiNbO_3$ high frequency microbalance.**

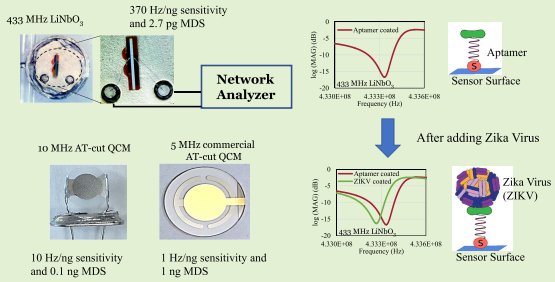

***Index Terms*—433 MHz Lithium Niobate crystal microbalance, whole virus sensor, Zika, aptamer.**

I. Introduction

ZIKA virus (ZIKV) pose a great danger as it spreads from a pregnant woman to the fetus causing birth defects like microcephaly and other congenital abnormalities. According to Vital Signs Report, around 14% of 1450 babies had Zika related health problems. It also causes Guillain-Barré syndrome, neuropathy and myelitis in adults. Hence early effective detection of Zika is necessary to control epidemic and as well as treatment. The different types of detection method of ZIKV includes serum analysis employing viral RNA or antibody-based detection assays [1], [2], molecular based detection assays like reverse transcription-polymerase chain reaction (RT-PCR)[3]–[9]. The molecular based detection method involves DNA extraction and then labelled detection using fluorescent probes, provides high sensitivity and specificity but at the same time requires specialized laboratory and expensive procedures. Aptamers are oligonucleotides that are designed to bind to specific sites of tissue, cells, pathogens and biomarkers. They are highly specific and unlike antigens that deteriorate as a function of time, they remain viable nearly indefinitely. When the aptamer binds to a specific target, its charge content shifts and changes, and its configuration may become different. These attributes along with the added mass and other changes that may occur in the mechanical [10], [11], optical [12], electrical [13]–[18] and thermal conductivity of the functionalized material or aptamer-target complex can be monitored to sense the target virus [19]. Here we use mechanical resonators coated with the Zika aptamer. When these surface-immobilized aptamers bind with Zika, the over-all mass loading on the resonator increases and affects its resonant frequency and bandwidth. To immobilize the aptamers on the microbalance, we used aptamers with a thiol (sulfur) linker that is known to covalently bind with gold and almost any other metals. We verified aptamer mass loading by measuring the resonator frequency shift after washing the aptamer-coated microbalance with de-ionized water. The same process was repeated after introducing the Zika virus. Fig. 1 shows the schematic of the Zika virus and the aptamer used to detect it. Zika virus is an RNA virus that belongs to the category of Flaviviridae, similar to Dengue virus, Japanese encephalitis virus, yellow fever virus and West Nile virus. The virus is a 40 nm diameter sphere with single capsid protein with lipid envelope having two membrane associated proteins (M and E) [20], [21],

Manuscript received November 1, 2019; revised December 13, 2019; accepted December 14, 2019. Date of publication December 23, 2019; date of current version March 17, 2020. This work was supported by the National Science Foundation (NSF) EAGER through Dr. Leon Esterowitz under Grant 1931100. The associate editor coordinating the review of this article and approving it for publication was Prof. Danilo Demarchi. *(Corresponding author: Massood Tabib-Azar.)*

Subhashish Dolai and Massood Tabib-Azar are with the Electrical and Computer Engineering Department, The University of Utah, Salt Lake City, UT 84112 USA (e-mail: subhashish.dolai@utah.edu; azar.m@utah.edu).

Digital Object Identifier 10.1109/JSEN.2019.2961611

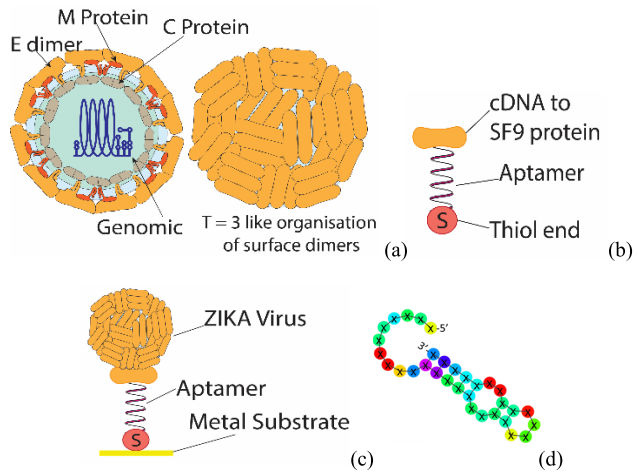

Fig. 1. Schematic of a) Zika virus, b) the aptamer with one end thiol and the other end a protein that attaches to the capsid protein of the Zika virus. c) Schematic of Zika virus attached to the aptamer immobilized on a gold substrate. d) The predicted schematic of folded structure of Aptamer (Image obtained from BasePair BioTechnology Inc).

schematically shown in the Fig. 1(a). The mass of single Zika virus is 43 kDa or 7.1×10^{-20} gm. The aptamers are artificially created single strand, DNA/RNA oligonucleotides used as recognition molecules for a target species. Aptamers are also called chemical antibodies and can be engineered to bind to specific proteins, amino acids, drugs, viruses with high specificity and affinity [22], [23]. The specific aptamer we used in our study was obtained from BasePair Biotechnologies Inc [24] and it consists of 32 nucleotide chain having molecular weight of 10 kDa (1.66×10^{-20} gm), that targets and binds with Zika SF9 envelope protein [25].

Quartz crystal microbalances (QCM) are piezoelectric resonators that are commonly used in measuring mass loading from the binding event. When an alternating electric field is applied, the inner dipole in the quartz crystal causes mechanical strain producing ultrasonic waves, resulting in crystal vibrating at a resonant frequency [26]. Their resonant frequency changes when mass is added to their surface. The sensitivity is described by the Sauerbrey equation [27] where the change in mass Δm on a certain area A, can be calculated from, $\Delta m/A = \Delta f_n(\rho_q\mu_q)^{0.5}/(-2nf_1^2)$, where, Δf_n is the change in resonant frequency, ρ_q is the density and μ_q is the shear modulus of quartz. AT-cut quartz is usually used because of its favorable temperature coefficient (±3 ppm/(−10 °C - +40 °C) [28] and its ability to operate in liquids due to its shear-mode vibration, enables it to be used in liquid applications. The Lithium Niobate oscillator (Fig. 2(a)) used in our work is a surface acoustic wave (SAW) device based on interdigitated electrode (IDT) demonstrated (Fig. 2(b)). The frequency of the SAW device is calculated from the distance between the electrodes in the IDT, and the frequency of operation is typically high (50 MHz – 5000 MHz), resulting in high mass sensitivity [29].

Atomic force microscopy (AFM) studies were done to show that aptamer sticks to gold surface and Zika on aptamer. Fig 3(a) shows the AFM scan image of Zika on aptamer

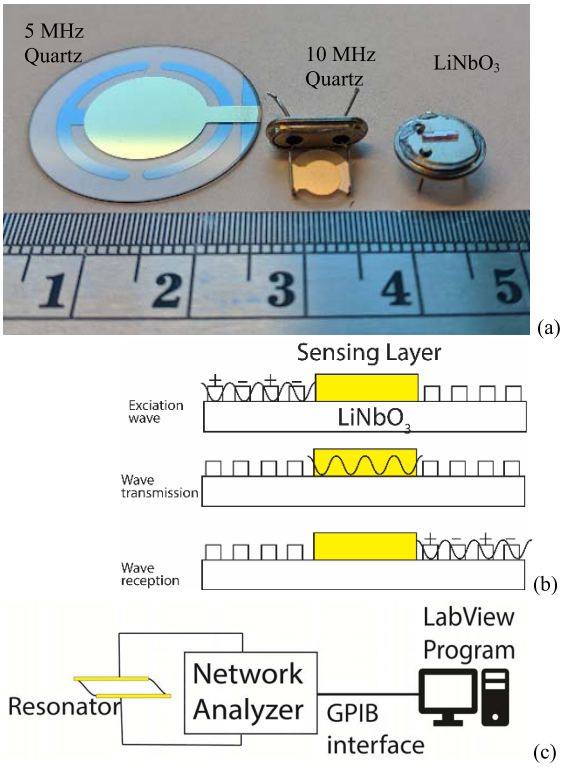

Fig. 2. Photograph of commercial 5 MHz quartz and 433 MHz Lithium Niobate (LiNbO3) microbalance sensors extracted from a) commercial filter (SFR433A). b): Schematic of the Standing Surface Acoustic Wave (S-SAW) sensor. The transducer converts the electrical energy from oscillating circuit to mechanical wave. c) Schematic of the microbalance measurement set-up.

on gold substrate, clearly showing the step height from the aptamer layer to Zika agrees with the dimension of a typical Zika virus. The minimum lateral lengths of ∼80 nm corresponding to two viruses with 40 nm height. The SEM image (Fig. 3(b)) also shows lateral lengths of ∼80 nm, which shows that the Zika agglomerate as they get immobilized on the surface coated with aptamer.

II. Experimental Procedure

The experiment was carried out on commercially available AT-cut gold coated 5 MHz quartz crystal (Fig. 2(a)) as a benchmark. Before preparing the sensor surface with the aptamer, the sensor was pretreated with acetone, ethanol followed by washing with DI water, successively and finally drying under nitrogen stream, in order to get rid of any contaminant from the surface. The resonant frequency of the crystal was measured using Agilent 4395A Network Analyzer, with the sensor fixed to inhouse made fixture. The resonant frequency was measured for 5 times with modified LabView program which extracts the resonant frequency from the spectrum data for 5 MHz commercial QCM (Fig. 4(a)), 10 MHz communication crystal (Fig. 4(b)) and 433 MHz $LiNbO_3$ SAW resonator (Fig. 4(c)). The instrument driver for Agilent 4395A Network Analyzer has been obtained from National Instruments website and then modified for added functionality to save the spectrum data along with

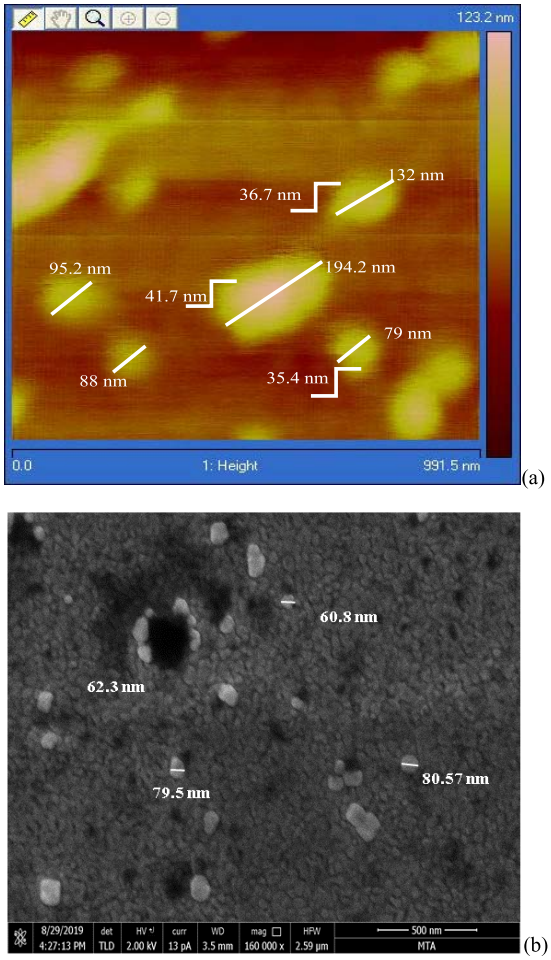

Fig. 3. a) AFM image of aptamer and Zika on gold substrate. Zika sits on aptamer with step height of ~40 nm. The lateral dimension shows that the zika is agglomerated in form of islands. The scale bar is 991.5 nm (b) SEM image of Zika on Aptamer. The scale bar is 500 nm.

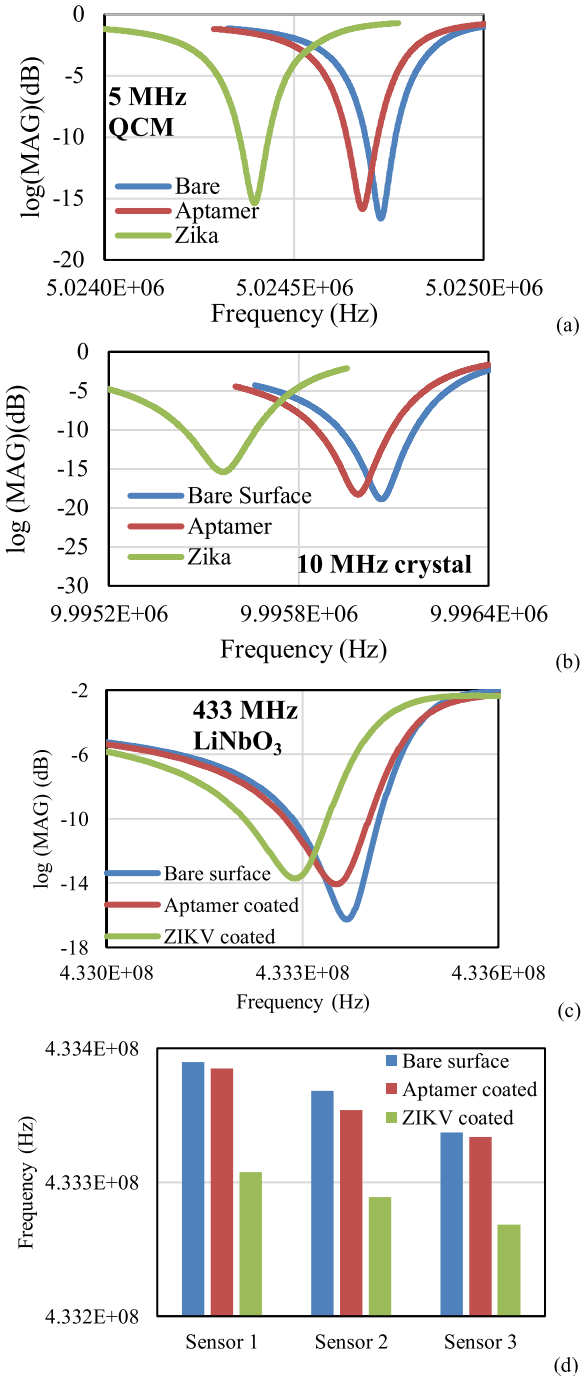

Fig. 4. Spectrum of (a) 5 MHz commercial QCM (b) 10 MHz communication crystal and (c) 433 MHz Lithium Niobate SAW sensor under pristine condition and after adding aptamer and Zika virus added. (d) Shift in center frequency of Lithium Niobate resonator repeated for 3 sensors.

the track and acquisition of resonant center frequency. The aptamers required activation for proper folding. The steps involved resuspension of the dried aptamer using resuspension buffer provided by BasePair Biotechnologies Inc. The aptamer solution was then diluted to 100 μM working concentration using Aptamer Folding Buffer (BasePair product), and then subsequently heated to 90°C −95 °C for 5 minutes and then cooled down to room temperature for 15 minutes. The 100 μM working aptamer was diluted to 1 μM solution using buffer solution. The buffer solution used is prepared with 1x concentration of Phosphate Buffer Saline (PBS) and 1 mM of magnesium chloride ($MgCl_2$). Then 2 μl of 1 μM thiol aptamer was dropped on the sensor surface and kept in hydrated container at 80°C for 10 minutes. The sensor was then dipped in DI water, to get rid-off the excess aptamer and blow dried in mild flow of nitrogen stream and 5 sets of resonant frequency measured in similar ways. This was repeated 3 times at different areas on the sensor with 2 μl at each time. After this 2 μl of stock inactivated ZIKV sourced from Zeptomatrix, was added to the aptamer coated sensor for 5 minutes to allow the binding with the aptamer and similarly dipped in DI water bath to get rid-of the excess and blow dried with mild stream of nitrogen and the shift in resonant frequency was measured (Fig 5(a) and (b)). The stock solution of Zika had a concentration of TCID50/ml titer [20], and the total number of Zika in 2 μl of stock solution was $\sim 3.5 \times 10^8$ estimated from the SEM image. Similar set of experiments were done for 10 MHz communication quartz crystal. The 10 MHz crystal was de-packaged and cleaned up as mentioned above and the resonant frequency was measured. For aptamer coating, 2 μl of 0.1 μM concentration was

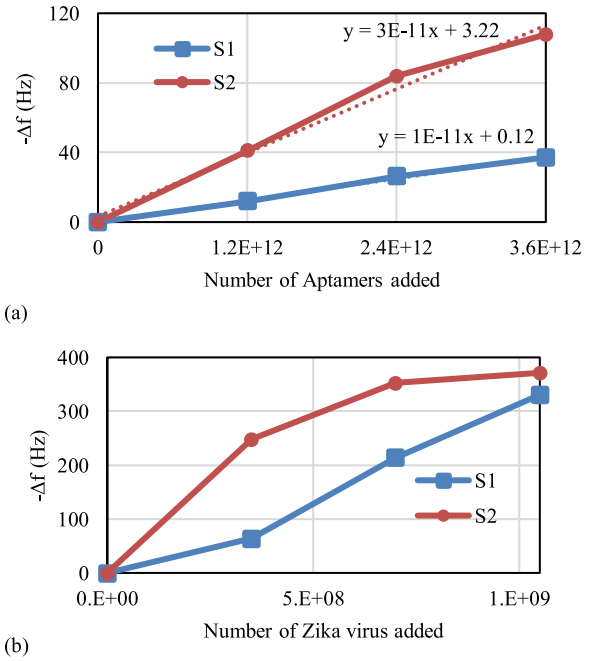

Fig. 5. a) and b) Δf as a function number of surface aptamers and Zika viruses on 5 MHz gold coated microbalance (S1 and S2).

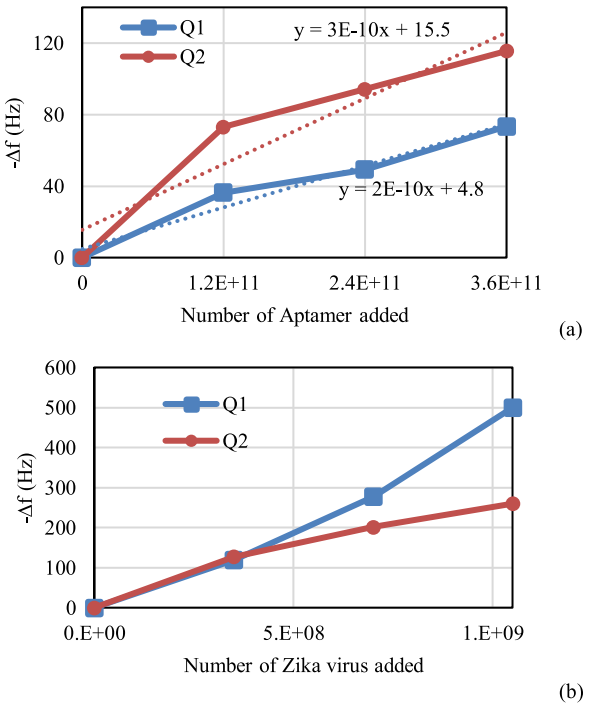

Fig. 6. Δf vs Δm with Aptamers a) and Zika viruses b) added on the sensor surface on 10 MHz quartz communication sensor (Q1 and Q2).

used for 1 minute and rinsed in water bath to remove the excess. Due to aggressive nature of the thiol end, any high concentration of thiol aptamer or prolonged exposure peels off the contact electrodes, rendering it useless. This was repeated in similar fashion for 3 different location on the sensor surface for both Aptamer and the ZIKV with the shift in resonant frequency ($-\Delta f$) response shown in Fig 6(a) and (b).

The measurements on the 433 MHz Lithium Niobate crystal was done similarly with 2 μl at each time for 3 times total and the ZIKV was added for one time only due to extremely small size of the sensor, as it spread throughout the sensor covering the whole aptamer coated surface. The spectrum and the resonant frequency have been shown for 5 MHz commercial QCM in Fig 4(a), 10 MHz communication crystal for Fig. 4(b) and Fig. 4(c) for each of the caseswhere aptamer and ZIKV was added a single time. The negative shift in resonant frequency implies the mass loading on the sensor surface after adding aptamer and Zika virus. Fig 4(d) shows the resonant frequency obtained for each after coating with aptamer and Zika virus and repeated for 3 different 433 MHz $LiNbO_3$ sensors. The reducing resonant frequency implies the increasing mass loading due to aptamer deposition on the sensor surface and Zika on aptamer. Each of the measurement was taken at IF bandwidth of 30 Hz with 800 points over a SPAN of 800 Hz for 5 MHz and 10 MHz crystal and 800 kHz for 433 MHz Lithium Niobate crystal.

III. Results and Discussion

Fig 5(a) shows the results of 5 MHz gold coated commercial sensor showing effect of adding mass to the sensor surface. The $-\Delta f$ was calculated with respect to the resonant frequency of the clean sensor. The increasing trend implies that the thiolated aptamer was attaching to the gold surface and thus immobilizing the aptamer. The number of aptamers has been calculated from the Avogadro number of molecules in 2 μl of the 1 μM thiol aptamer solution, which corresponds to the number 1.2×10^{12}. The mass of each Aptamer is $\sim$ 10 kDa which results in 19.2 ng for each 2 μl of 1 μM Aptamer solution. The average sensitivity obtained from the results of the 2 sensors was $\sim$1 Hz/ng obtained by eliminating the noise floor [30]. Each of the points in every 2 μl added was an average of five measurements.

The typical maximum shift in the frequencies from the average of 5 measurements was $\sim$ 2Hz. The sensor response to zika virus is shown in Fig 5(b), which shows an increase in Δf shift with each time addition of 2 μl of stock zika solution which corresponds to $\sim 2 \times 10^{-11}$ gm of Zika virus. However, the frequency shift is much higher than the Aptamer number, which can be explained by probable deposition of residue from virus suspension solution that came with the stock Zika, on the sensor surface. Fig 6(a) and 6(b) shows results of the 10 MHz commercial communication quartz crystal. The 10 MHz crystal had a higher sensitivity of 10 Hz/ng, with an average maximum error of $\sim$1 Hz in measurement of the resonant frequencies. The sensor response S2 in Fig 5 and Q2 in Fig 6 saturates as the analytes (aptamer/Zika) are added in successive steps, because of the overlapping coverage of the analyte on the sensor surface. Hence, the successive addition of analyte on the sensor surface after the first instance, only deposited a little mass on the sensor surface.

Figures 7 (a) and (b) show the results of the 433 MHz Lithium Niobate crystal. The trends are similar to that of the gold coated 5MHz as well as 10 MHz crystal hence clearly showcasing that the thiolated aptamers are binding

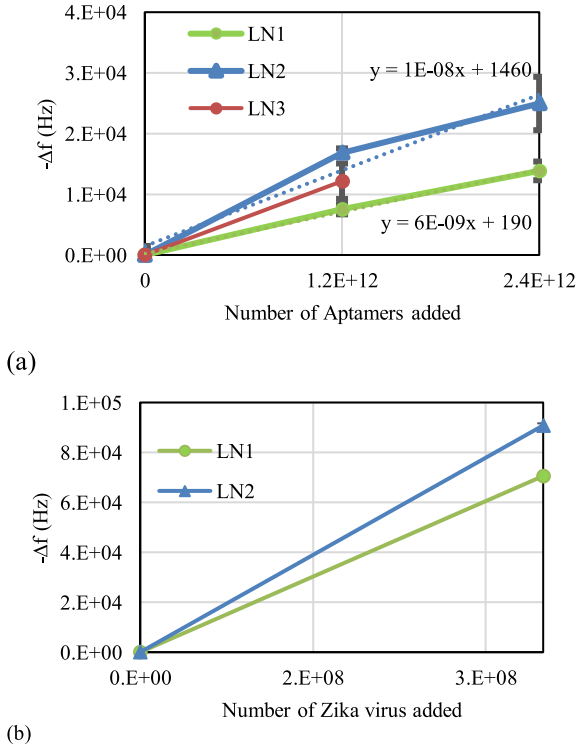

Fig. 7. $-\Delta f$ vs m with Aptamers a) and Zika viruses b) added on the sensor surface 433 MHz Lithium Niobate communication crystal (LN1 and LN2).

to the metallic electrodes on the surface. The relatively high resonant frequency resulted in average shift in frequency of ∼480x more than the 5 MHz crystal and ∼203x more than the 10 MHz crystal for the same amount of Aptamer added. This resulted in increased sensitivity to ∼370 Hz/ng which is improved by a factor of ∼400x than the 5 MHz commercial crystal. The average error shift in resonant frequency was ∼900 Hz. The response of sensor LN3 was limited to the first aptamer coating as, due to aggressive nature of the thiol end of the aptamer, peeling off the metallic contact on the surface, rendering the sensor useless. The same results were obtained using the 10 MHz quartz crystal.

The response to the Zika for both the 10 MHz quartz communication crystal (Fig. 6(b)) and 433 MHz Lithium Niobate crystal (Fig 7(b)) is similar to that of the 5 MHz commercial sensor with much higher frequency shift than the approximate number of Zika added each time. The probable cause has been discussed in the previous section. The slope obtained by linear fitted curve shows near similar characteristics for corresponding sensor concerned.

The frequency response of the commercial 5 MHz crystal and 10 MHz communication crystal was measured with 801 points and the SPAN was set to 800 Hz over the resonant center frequency at an IF Bandwidth of 30 Hz. This provided a minimum detectable frequency shift to 800/801 Hz ≈ 1 Hz. Hence, from the previously discussed results of the 5 MHz and 10 MHz crystal, the minimum detectable signal (MDS) is the mass loading corresponding to 1 Hz shift in the resonant frequency, which is 1 ng and 0.1 ng, respectively. For the Lithium Niobate, all other measurement parameters are similar except the SPAN of 800 kHz was used. Hence, the step size in the frequency spectrum for each point is 800 kHz/801 ≈ 998 Hz. However, the IF bandwidth used for measuring the spectrum is 30 Hz, which divides the span of the frequency into small segments of 30 Hz and measuring the frequency response, providing high resolution and stable output response. Hence the minimum mass loading can be considered for 1 Hz shift.

IV. Conclusion

This paper demonstrates the use of Lithium Niobate communication resonator for the first time as a very sensitive whole virus detector with ∼ 400 times better sensitivity than typical commercial 5 MHz quartz microbalance. The thiolated aptamer binds to the surface electrode of the Lithium Niobate microbalance making it target specific to bind to zika viruses. This could be generalized to any whole virus sensor provided the aptamer is engineered to detect the target virus.

Acknowledgment

The authors would like to thank contributions of Dr. J. Magda and Dr. T. Nguyen, Chemical Engineering Department, University of Utah, for Aptamer activation and Zika virus handling and processing.

References

[1] C. J. Haug, M. P. Kieny, and B. Murgue, "The zika challenge," *New England J. Med.*, vol. 374, no. 19, pp. 1801–1803, 2016.
[2] A. A. Al-Qahtani, N. Nazir, M. R. Al-Anazi, S. Rubino, and M. N. Al-Ahdal, "Zika virus: A new pandemic threat," *J. Infection Developing Countries*, vol. 10, no. 3, pp. 201–207, 2016.
[3] D. Musso, C. Roche, T.-X. Nhan, E. Robin, A. Teissier, and V. M. Cao-Lormeau, "Detection of Zika virus in saliva," *J. Clin. Virol.*, vol. 68, pp. 53–55, Jul. 2015.
[4] C. Klungthong *et al.*, "Dengue virus detection using whole blood for reverse transcriptase PCR and virus isolation," *J. Clin. Microbiol.*, vol. 45, no. 8, pp. 2480–2485, Aug. 2007.
[5] A.-C. Gourinat, O. O'Connor, E. Calvez, C. Goarant, and M. Dupont-Rouzeyrol, "Detection of Zika virus in urine," *Emerg. Infectious Diseases*, vol. 21, no. 1, pp. 84–86, Jan. 2015.
[6] O. Faye, O. Faye, A. Dupressoir, M. Weidmann, M. Ndiaye, and A. A. Sall, "One-step RT-PCR for detection of Zika virus," *J. Clin. Virol.*, vol. 43, no. 1, pp. 96–101, 2008.
[7] G. Calvet *et al.*, "Detection and sequencing of Zika virus from amniotic fluid of fetuses with microcephaly in Brazil: A case study," *Lancet Infectious Diseases*, vol. 16, pp. 653–660, Jun. 2016.
[8] K. O. Murray *et al.*, "Prolonged detection of Zika virus in vaginal secretions and whole blood," *Emerg. Infectious Diseases*, vol. 23, no. 1, pp. 99–101, Jan. 2017.
[9] J. Shin, A. G. Cherstvy, and R. Metzler, "Sensing viruses by mechanical tension of DNA in responsive hydrogels," *Phys. Rev. X*, vol. 4, no. 2, 2014, Art. no. 021002.
[10] B. Ilic, Y. Yang, and H. G. Craighead, "Virus detection using nanoelectromechanical devices," *Appl. Phys. Lett.*, vol. 85, no. 13, pp. 2604–2606, Sep. 2004.
[11] P. Negri *et al.*, "Direct optical detection of viral nucleoprotein binding to an anti–influenza aptamer," *Anal. Chem.*, vol. 84, no. 13, pp. 5501–5508, Jul. 2012.
[12] H. M. So *et al.*, "Detection and titer estimation of *Escherichia coli* using aptamer-functionalized single-walled carbon-nanotube field-effect transistors," *Small*, vol. 4, no. 2, pp. 197–201, 2008.
[13] A. R. Ruslinda, X. Wang, Y. Ishii, Y. Ishiyama, K. Tanabe, and H. Kawarada, "Human immunodeficiency virus trans-activator of transcription peptide detection via ribonucleic acid aptamer on aminated diamond biosensor," *Appl. Phys. Lett.*, vol. 99, no. 12, 2011, Art. no. 123702.

[14] K. Maehashi, T. Katsura, K. Kerman, Y. Takamura, K. Matsumoto, and E. Tamiya, "Label-free protein biosensor based on aptamer-modified carbon nanotube field-effect transistors," *Anal. Chem.*, vol. 79, no. 2, pp. 782–787, Jan. 2007.
[15] Y. Ohno, K. Maehashi, and K. Matsumoto, "Label-free biosensors based on aptamer-modified graphene field-effect transistors," *J. Amer. Chem. Soc.*, vol. 132, no. 51, pp. 18012–18013, Dec. 2010.
[16] R. A. Rahim, K. Tanabe, S. Ibori, X. Wang, and H. Kawarada, "Effects of diamond-FET-based RNA aptamer sensing for detection of real sample of HIV-1 tat protein," *Biosensors Bioelectron.*, vol. 40, pp. 277–282, Feb. 2013.
[17] K. S. Kim, H. S. Lee, J. A. Yang, M. H. Jo, and S. K. Hahn, "The fabrication, characterization and application of aptamer-functionalized Si-nanowire FET biosensors," *Nanotechnology*, vol. 20, May 2009, Art. no. 235501.
[18] M. Jenik *et al.*, "Sensing picornaviruses using molecular imprinting techniques on a quartz crystal microbalance," *Anal. Chem.*, vol. 81, no. 13, pp. 5320–5326, Jul. 2009.
[19] R. N. Charrel, I. Leparc-Goffart, S. Pas, X. de Lamballerie, M. Koopmans, and C. Reusken, "Background review for diagnostic test development for Zika virus infection," *Bull. World Health Org.*, vol. 94, pp. 574–584, Aug. 2016.
[20] P. Leyssen, E. de Clercq, and J. Neyts, "Perspectives for the treatment of infections with flaviviridae," *Clin. Microbiol. Rev.*, vol. 13, no. 1, pp. 67–82, Jan. 2000.
[21] K. H. Lee and H. Zeng, "Aptamer-based ELISA assay for highly specific and sensitive detection of Zika NS_1 protein," *Anal. Chem.*, vol. 89, no. 23, pp. 12743–12748, Dec. 2017.
[22] R. D. Jenison, S. C. Gill, A. Pardi, and B. Polisky, "High-resolution molecular discrimination by RNA," *Science*, vol. 263, pp. 1425–1429, Mar. 1994.
[23] Base Pair Biotechnologies. *Base Pair Biotechnologies—Aptamer Discovery Company*. [Online]. Available: https://www.basepairbio.com/
[24] Prospec Protein Specialists. *Zika Envelope Recombinant Antigen | Zika Virus | ProSpec*. [Online]. Available: https://www.prospecbio.com/zika_envelope_sf9
[25] K. Bizet, C. Gabrielli, and H. Perrot, "Biosensors based on piezolectric transducers," *Analusis*, vol. 27, pp. 609–616, 1999.
[26] G. Sauerbrey, "Verwendung von schwingquarzen zur wägung dünner schichten und zur mikrowägung," *Zeitschrift Phys.*, vol. 155, no. 2, pp. 206–222, 1959.
[27] V. Matko, "A comparison of frequency pullability in oscillators using a single AT-cut quartz crystal and those using two single AT-cut crystals connected in parallel with a series load capacitance or series load inductance," *Sensors*, vol. 6, pp. 746–755, Jul. 2006.
[28] S. J. Martin, G. C. Frye, and S. D. Senturia, "Dynamics and response of polymer-coated surface acoustic wave devices: Effect of viscoelastic properties and film resonance," *Anal. Chem.*, vol. 66, no. 14, pp. 2201–2219, Jul. 1994.
[29] F. L. Dickert, P. Forth, W.-E. Bulst, G. Fischerauer, and U. Knauer, "SAW devices-sensitivity enhancement in going from 80 MHz to 1 GHz," *Sens. Actuators B, Chem.*, vol. 46, no. 2, pp. 120–125, Feb. 1998.

Subhashish Dolai received the master's degree in VLSI design from the Indian Institute of Engineering Science and Technology, Shibpur, India. He is currently pursuing the Ph.D. degree with the University of Utah, UT, USA.

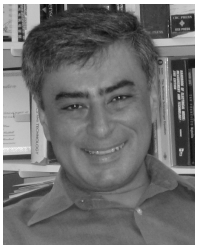

Massood Tabib-Azar (Senior Member, IEEE) received the M.S. and Ph.D. degrees in electrical engineering from the Rensselaer Polytechnic Institute in 1984 and 1986, respectively.

In 1987, he joined the Faculty of the EECS Department, Case Western Reserve University. He was a Fellow with NASA from 1992 to 1992, on Sabbatical with Harvard University from 1993 to 1994, with Yale University from 2000 to 2001, with UC Berkeley from 2015 to 2016, and with the Massachusetts Institute of Technology in 2016. He was a Program Director with the ECCS Division of National Science Foundation from 2012 to 2013. He is currently a USTAR Professor of ECE with the Electrical and Computer Engineering Department, University of Utah, with an adjunct appointment in Bioengineering Department. His current research interests include nanometrology, micro-plasma devices, nano-electromechanical computers, novel devices based on solid electrolytes (memristors), sensors and actuators, injectable bio-systems, quantum sensing, and quantum computing. His teaching interests include development of courses in the area of electronic device physics and electromagnetics with an emphasis on solving problems and the use of computer-aided instruction tools. He is the author of three books, two book chapters, more than 200 journal publications, and numerous conference proceeding articles. He has introduced and chairs many international symposia in his fields of interest. Dr. Tabib-Azar is a member of the New York Academy of Sciences, IEEE (Electron Devices), APS, AAPT, and Sigmai Xi research societies. He was a recipient of the 1991 Lilly Foundation Fellowship. He has received more than 14 certificate of appreciation and recognition for his professional activities and the Best Paper Award from Design Automation Conference in 2001 for his work on electromagnetic properties of interconnects and defects in ICs, the Best Paper Award from International Conference on Intelligent Robots and Systems in 2004 for his work on human–machine interface, and the Best Paper Award from ISQED for his work on NEMS Processors, in 2011. He is in the Editorial Board of the IEEE ELECTRON DEVICE LETTERS.